

# Dorsal activity of maternal *squint* is mediated by a non-coding function of the RNA

Shimin Lim<sup>1,2</sup>, Pooja Kumari<sup>1,3</sup>, Patrick Gilligan<sup>1</sup>, Helen Ngoc Bao Quach<sup>1</sup>, Sinnakaruppan Mathavan<sup>4</sup> and Karuna Sampath<sup>1,2,3,\*</sup>

## SUMMARY

Despite extensive study, the earliest steps of vertebrate axis formation are only beginning to be elucidated. We previously showed that asymmetric localization of maternal transcripts of the conserved zebrafish TGF $\beta$  factor Squint (Sqt) in 4-cell stage embryos predicts dorsal, preceding nuclear accumulation of  $\beta$ -catenin. Cell ablations and antisense oligonucleotides that deplete Sqt lead to dorsal deficiencies, suggesting that localized maternal *sqt* functions in dorsal specification. However, based upon analysis of *sqt* and Nodal signaling mutants, the function and mechanism of maternal *sqt* was debated. Here, we show that *sqt* RNA may function independently of Sqt protein in dorsal specification. *sqt* insertion mutants express localized maternal *sqt* RNA. Overexpression of mutant/non-coding *sqt* RNA and, particularly, the *sqt* 3'UTR, leads to ectopic nuclear  $\beta$ -catenin accumulation and expands dorsal gene expression. Dorsal activity of *sqt* RNA requires Wnt/ $\beta$ -catenin but not Oep-dependent Nodal signaling. Unexpectedly, *sqt* ATG morpholinos block both *sqt* RNA localization and translation and abolish nuclear  $\beta$ -catenin, providing a mechanism for the loss of dorsal identity in *sqt* morphants and placing maternal *sqt* RNA upstream of  $\beta$ -catenin. The loss of early dorsal gene expression can be rescued by the *sqt* 3'UTR. Our findings identify new non-coding functions for the Nodal genes and support a model wherein *sqt* RNA acts as a scaffold to bind and deliver/sequester maternal factors to future embryonic dorsal.

**KEY WORDS:** 3'UTR, Axis formation, Dorsal localization, Dorsal expansion, Maternal factors, Non-coding RNA, Nodal, RNA localization, Squint (Nodal-related 1), Zebrafish

## INTRODUCTION

The specification of the embryonic axes in many organisms is initiated by maternally deposited factors that activate various signaling pathways to establish the body plan. In *Drosophila*, frogs and fish, asymmetric localization of maternal factors in oocytes and eggs is crucial for correct embryonic patterning (St Johnston, 1995; Grunert and St Johnston, 1996; Mowry and Cote, 1999; Pelegri, 2003; Heasman, 2006; Abrams and Mullins, 2009; Nojima et al., 2010; Lu et al., 2011). In *Xenopus*, *wnt11* RNA is localized in dorsal vegetal cells, and blocking maternal Wnt and  $\beta$ -catenin functions leads to dorsal deficiencies (Heasman et al., 1994; Wylie et al., 1996; Schroeder et al., 1999; Heasman et al., 2000; Kofron et al., 2001; Tao et al., 2005). Recent work has also implicated vegetally localized Trim36 ubiquitin ligase in microtubule-dependent cortical rotation and axis formation (Cuykendall and Houston, 2009).

In zebrafish, several experiments have suggested that dorsal determinants are vegetally localized, and are translocated via microtubules to trigger dorsal axis specification (Jesuthasan and Strahle, 1997; Mizuno et al., 1999; Ober and Schulte-Merker, 1999). The molecular nature of the maternal factors is just beginning to be elucidated (Abrams and Mullins, 2009). We previously showed that maternal RNA encoding the Nodal morphogen Squint [Sqt; Nodal-related 1 (Ndr1) – Zebrafish

Information Network] asymmetrically localizes in two cells of 4-cell stage embryos (Gore and Sampath, 2002; Gore et al., 2005), and predicts embryonic dorsal prior to the nuclear accumulation of  $\beta$ -catenin in dorsal cells. Removal of *sqt* RNA-containing (*sqt*<sup>+</sup>) cells and knockdown by antisense morpholino oligonucleotides leads to dorsal deficiencies, suggesting that asymmetrically localized maternal *sqt* functions in dorsal specification.

Paradoxically, females homozygous for the *sqt* insertion mutations *sqt*<sup>cz35</sup> and *sqt*<sup>hi975</sup> (Heisenberg and Nusslein-Volhard, 1997; Erter et al., 1998; Feldman et al., 1998; Amsterdam et al., 2004) produce embryos with mild dorsal deficiencies and do not manifest the loss of anterior and dorsal structures observed upon depletion of *sqt*, either by antisense morpholinos or embryological dissections of *sqt*<sup>+</sup> cells (Aoki et al., 2002; Bennett et al., 2007; Pei et al., 2007). Similarly, maternal and zygotic mutations affecting the Nodal co-receptor *one-eyed pinhead* (*oep*) (Gritsman et al., 1999) result in embryos similar to zygotic *cyc*; *sqt* double mutants (*cyc* is also known as *ndr2* – Zebrafish Information Network) (Feldman et al., 1998; Dougan et al., 2003), but these embryos do not manifest complete loss of anterior or dorsal structures. Therefore, the function of maternal *sqt* has been a matter of debate (Bennett et al., 2007; Gore et al., 2007).

Using several mutations that disrupt Sqt, we find that *sqt* RNA has functions independent of Sqt protein in dorsal initiation. Furthermore, our analysis shows that the *sqt*<sup>cz35</sup> and *sqt*<sup>hi975</sup> insertion alleles, on which the genetic analysis was based, still express and localize maternal *sqt* transcripts, similar to wild-type embryos. We demonstrate that mutant RNAs still have dorsal-inducing activity in embryos, and show that this activity is a non-coding function of *sqt* RNA. Interestingly, the non-coding, dorsal-inducing activity of *sqt* RNA is dependent on sequences within its 3'UTR. We also revisited the activity of *sqt* morpholinos, and find that *sqt* translation initiation site sequences are also required for *sqt*

<sup>1</sup>Temasek Life Sciences Laboratory, 1 Research Link, National University of Singapore, Singapore 117604. <sup>2</sup>School of Biological Sciences, Nanyang Technological University, 60 Nanyang Drive, Singapore 637551. <sup>3</sup>Department of Biological Sciences, National University of Singapore, 14 Science Drive, Singapore 117543. <sup>4</sup>Genome Institute of Singapore, 60 Biopolis Street, Genome, Singapore 138672.

\*Author for correspondence (karuna@tll.org.sg)

RNA localization. The dorsal-inducing activity of *sqt* RNA is independent of Sqt/Nodal signaling, but requires functional maternal Wnt/ $\beta$ -catenin signaling. Our findings identify novel non-coding functions for the Nodal genes and reveal new roles for non-coding RNAs in the maternal control of axis specification.

## MATERIALS AND METHODS

### Generation of constructs

pCS2+*sqt*<sup>STOP</sup>, pCS2+FLAG*sqt* and pCS2+FLAG*sqt*<sup>STOP</sup> were generated by PCR-based site-directed mutagenesis. pCS2+*sqt*<sup>STOP</sup> and pCS2+FLAG*sqt* were generated using pCS2+*sqt* (Gore et al., 2005) as PCR template, whereas pCS2+FLAG*sqt*<sup>STOP</sup> was generated from pCS2+*sqt*<sup>STOP</sup>. pCS2+*sqt*<sup>cz35</sup> was generated by amplifying two overlapping fragments from *MZsqt*<sup>cz35</sup> cDNA, followed by overlap extension PCR and subcloning into pCS2+. pCS2+T-*sqt* was generated using pCS2+*sqt*<sup>cz35</sup> as PCR template, followed by subcloning into pCS2+. Primers are listed in supplementary material Table S1.

### Zebrafish strains

Wild-type zebrafish, *MZsqt*<sup>cz35</sup>, *MZsqt*<sup>hi975</sup>, *MZdicer*<sup>hu715</sup>, *MZoepe*<sup>z57</sup> and homozygous *ich*<sup>h1</sup> mutant fish were maintained at 28.5°C and embryos were obtained by natural mating using standard procedures, in accordance with institutional animal care regulations (Westerfield, 2007). The genotype of *MZsqt*<sup>cz35</sup> embryos was determined as described (Feldman et al., 1998). Homozygous *ich* mutant mothers that yielded 100% radialized embryos were used and identified as described (Kelly et al., 2000; Bellipanni et al., 2006).

### Quantitative real-time RT-PCR

Total RNA was extracted from embryos using TRIzol reagent (Invitrogen). 250 ng RNA from WT, *MZsqt*<sup>hi975</sup> and *MZsqt*<sup>cz35</sup> embryos and 250 ng RNA from lacZ:glor or lacZ:*sqt* RNA-injected embryos was used for cDNA synthesis. 1  $\mu$ l first-strand cDNA was used in 10  $\mu$ l PCR reactions. Genomic DNA contamination was checked by PCR to detect *actb2* (*act*), *sqt*, *dharma* (*dha*; *bozozok*), *vox* and *vent*. Primers are listed in supplementary material Table S1. RT-PCR was performed on an ABI 7900HT Fast Real-Time PCR System (Applied Biosystems) using the comparative C<sub>T</sub> method. Control experiments to measure changes in C<sub>T</sub> with template dilutions were performed to test whether amplification efficiencies of target (*sqt*, *dha*, *vox* and *vent*) and control (*act*) primers were similar. All results were normalized to *act*.

### Capped mRNA synthesis, injections and in situ hybridizations

Capped mRNA was synthesized from linearized plasmids (*NotI*, NEB) using the SP6 mMessage mMachine Kit (Ambion), and 25 pg aliquots were injected into 1-cell stage embryos. Fluorescent Alexa 488-labeled RNA was synthesized, injected at the 1-cell stage (Gore et al., 2005; Gilligan et al., 2011) and RNA localization scored visually (Gilligan et al., 2011) by two individuals independently.

To target maternal *sqt* RNA prior to the formation of *sqt* RNA aggregates that develop upon egg activation (Gore and Sampath, 2002), 10 ng aliquots of control or *sqt* morpholinos were injected into squeezed wild-type eggs and fertilized with wild-type sperm (Gore et al., 2005; Gore et al., 2007). Injected embryos were fixed in 4% paraformaldehyde/PBS at oblong, sphere, dome, 30% epiboly, 40% epiboly, 50% epiboly, 60% epiboly and at 24 hours post-fertilization (hpf), and processed for whole-mount in situ hybridization to detect *gooseoid*, *chordin*, *gata2* and *no tail* (Sampath et al., 1998). Localization of *sqt* RNA was detected by in situ hybridization using full-length cDNA probes.

### In vitro translation and protein detection

The TNT® SP6 Coupled Rabbit Reticulocyte Lysate System (Promega) was used to transcribe and translate from the following plasmid templates: pCS2+, pCS2+*sqt*FL:*sqt*, pCS2+*sqt*<sup>STOP</sup>, pCS2+*sqt*<sup>cz35</sup>, pCS2+FLAG*sqt*, pCS2+FLAG*sqt*<sup>STOP</sup> and pCS2+T-*sqt*. 1  $\mu$ g of plasmid DNA was used in 50  $\mu$ l reactions according to the manufacturer's instructions (Promega). Biotin-labeled protein products were separated by SDS-PAGE and transferred onto Hybond-C Extra membranes (GE Healthcare).

Immunoblotting was performed using avidin and biotinylated HRP (1:200 dilution) (Ultra-sensitive ABC Peroxidase Rabbit IgG Staining Kit, Pierce). Proteins were detected by Kodak Biomax MS film using SuperSignal West Fento Maximum Sensitivity Substrate (Pierce). FLAG epitope-tagged peptides were detected with anti-FLAG M2 mouse monoclonal primary antibody (1:2500, Sigma) and HRP-conjugated anti-mouse IgG secondary antibody (1:5000, DAKO). To detect nuclear  $\beta$ -catenin, 512-cell stage embryos were fixed in 4% paraformaldehyde/PBS and processed for fluorescence immunohistochemistry using a rabbit polyclonal anti- $\beta$ -catenin antibody (C2206, Sigma) and Alexa 488-conjugated goat anti-rabbit secondary antibodies (Molecular Probes).

To compare translation efficiencies of Sqt:glor UTR and Sqt:*sqt* UTR, 1-cell stage wild-type embryos were injected with 20 pg *sqt*-GFP:glor or *sqt*-GFP:*sqt*. Approximately 40–50 injected embryos were manually dechorionated and lysed at 50% epiboly in RIPA buffer. Whole embryo lysates (50  $\mu$ g/lane) were separated by SDS-PAGE and transferred onto Hybond-C Extra membranes. Proteins were detected on film as described above. Sqt-GFP was immunoblotted using rabbit polyclonal anti-GFP antibodies (1:2500, Abcam), followed by HRP-conjugated anti-rabbit IgG secondary antibodies (1:5000, DAKO). Tubulin was detected using mouse monoclonal anti-tubulin antibodies (1:2500, Sigma), followed by HRP-conjugated anti-mouse IgG secondary antibodies.

### Microscopy

Live embryos injected with fluorescent RNAs or expressing Sqt-GFP fusion protein were manually dechorionated, mounted in 2.5% methylcellulose (Sigma) and visualized using a Zeiss Axioplan2 microscope with a CoolSNAP HQ camera (Photometrics). MetaMorph (Universal Imaging Corporation) and ImageJ (NIH) software packages were used to acquire and process images. Stained embryos from in situ hybridization and immunohistochemistry experiments were mounted in 100% glycerol and imaged using a Zeiss Axioplan2 microscope equipped with a Nikon DXM1200 color camera. Images were acquired using ACT-1 software (Nikon) and cropped using Adobe Photoshop.

For  $\beta$ -catenin- and DAPI-stained embryos, images were acquired using a Zeiss LSM 5 Exciter upright confocal microscope. To quantify  $\beta$ -catenin-positive nuclei, 15–25 optical sections at 1.76  $\mu$ m intervals starting from the yolk syncytial layer nuclei were examined per embryo. We detected  $\beta$ -catenin-positive nuclei in many sections. However, owing to intense membrane and cytoplasmic  $\beta$ -catenin staining that obscured nuclear staining upon z-projection of all sections obtained, three serial confocal sections for each embryo were selected, z-projected using LSM Image Browser software, and cropped using Adobe Photoshop.

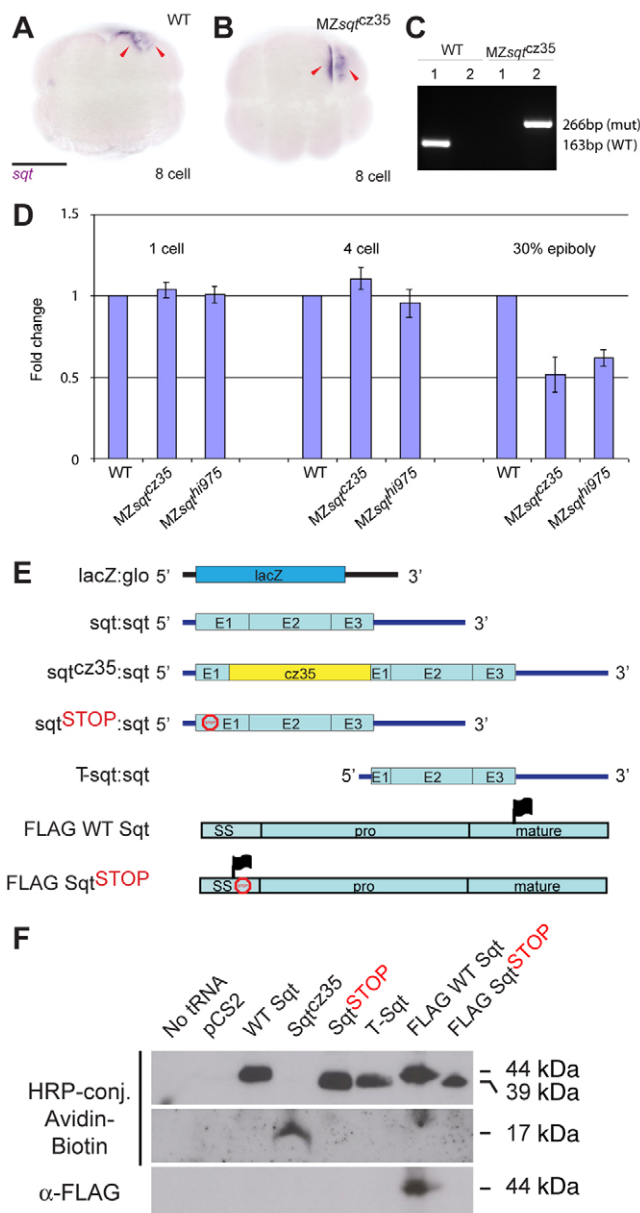
### Measurement of expression domains

Animal pole view images of embryos stained for *gsc* were used. In ImageJ, we drew a best-fit circle for the circumference of the embryo using the Circle tool. Using the xy coordinates, the diameter of the circle along the x- and y-axes and its center were determined. The Radial Grid tool in ImageJ and the center coordinates were used to mark the center, and using the Angle and Measure tools the angle of *gsc* expression was determined.

## RESULTS

### Mutant *sqt* RNA expands dorsal gene expression in early embryos

To examine whether the insertion mutants had any *sqt* activity, we first determined if the RNA and protein are expressed. We previously showed that embryos from fish homozygous for the *sqt*<sup>cz35</sup> and *sqt*<sup>hi975</sup> insertions express maternal *sqt* RNA (Gore et al., 2007). Whole-mount in situ hybridizations show that, similar to wild-type embryos, mutant *sqt* RNA is localized to two cells at the 4- and 8-cell stage in *MZsqt* mutant embryos (Fig. 1A–C; genotypes confirmed by PCR, Fig. 1C). Quantitative PCRs show that *MZsqt* mutant and wild-type embryos have similar levels of maternal *sqt* RNA at the 1-cell and 4-cell stages, and that a decrease in *sqt* RNA levels occurs in *MZsqt* mutant embryos later during gastrulation (Fig. 1D). Similar to wild-type embryos, we



detect non-polyadenylated mutant *sqt* RNA that is spliced as well as unspliced in pd(N)<sub>6</sub>-primed cDNA from 4-cell stage embryos, whereas only spliced *sqt* RNA is detected using oligo(dT)-primed cDNA (supplementary material Fig. S1A,B). These results show that mutant maternal *sqt* RNA is expressed and localized to future dorsal cells in MZ*sqt* mutant embryos at levels similar to wild-type embryos. Therefore, the *sqt* insertion alleles are not maternal transcript nulls, and maternal *sqt* RNA levels in mutant embryos are similar to those in wild-type embryos.

To test whether the *sqt*<sup>cz35</sup> insertion RNA generates any Sqt protein, we expressed sqt<sup>cz35</sup>:sqt RNA in a rabbit reticulocyte lysate expression system. The insertion RNA is predicted to encode a 17 kDa C-terminally truncated peptide lacking any functional ligand. We find that protein expressed from sqt<sup>cz35</sup>:sqt RNA is the predicted 17 kDa peptide (Feldman et al., 1998). We also tested synthetic *sqt* RNA with a stop codon in the first exon (TTG>TAG, which results in Leu11>STOP; sqt<sup>STOP</sup>:sqt), a truncated *sqt* RNA (T-sqt:sqt) (Bennett et al., 2007), and FLAG epitope-tagged

**Fig. 1. Mutant *sqt* RNAs are expressed and localized in MZ*sqt* mutant zebrafish embryos.** (A,B) Whole-mount in situ hybridization to detect localization of maternal *sqt* RNA (arrowheads) in 8-cell stage wild-type (WT) (A) and MZ*sqt*<sup>cz35</sup> mutant (B) embryos. (C) The genotype of wild-type (A) and MZ*sqt*<sup>cz35</sup> (B) embryos was confirmed by PCR to detect either wild-type (primer pair 1) or mutant *sqt* (primer pair 2) alleles. (D) Quantitative PCR to detect *sqt* RNA shows that maternal *sqt* transcript levels in MZ*sqt* mutants are similar to those of wild-type embryos at the 1-cell and 4-cell stages, and that reduced *sqt* transcript levels are observed at gastrula stages in the mutant. Error bars indicate s.d. between three independent experiments. (E) Schematic of constructs to express *lacZ*, wild-type *sqt* (WT Sqt), *sqt*<sup>cz35</sup> (Sqt<sup>cz35</sup>), *sqt* with a terminator codon in exon 1 (Sqt<sup>STOP</sup>), a 5' truncation of *sqt* (T-Sqt), and FLAG epitope-tagged wild-type *sqt* (FLAG WT Sqt) and Sqt<sup>STOP</sup> (FLAG Sqt<sup>STOP</sup>) in rabbit reticulocyte lysates (as shown in F). *sqt* coding sequences are in cyan (exons are indicated as E1-3), with the *sqt*<sup>cz35</sup> insertion in yellow. Black line indicates *globin* 3'UTR sequences and the blue line indicates the *sqt* UTRs. Red octagons indicate the position of the terminator codon in Sqt<sup>STOP</sup> and FLAG Sqt<sup>STOP</sup> and black flags mark the position of the FLAG epitope tags. SS, signal sequence. (F) In vitro translation to express Sqt proteins from the constructs described in E showing the expected 44 kDa wild-type Sqt protein, a C-terminus truncated 17 kDa Sqt<sup>cz35</sup> peptide, and that both Sqt<sup>STOP</sup> and T-sqt produce the predicted 39 kDa protein from Met35. Scale bar: 100 μm.

versions of wild-type Sqt and Sqt<sup>STOP</sup> (Fig. 1E). Translation from control and FLAG-tagged *sqt* RNA showed the expected 44 kDa proteins, whereas translation from sqt<sup>STOP</sup>:sqt and T-sqt:sqt RNA yielded an N-terminally truncated peptide of 39 kDa, lacking the signal sequence (Fig. 1E,F). In this in vitro translation system, the peptide from sqt<sup>STOP</sup>:sqt presumably results from utilization of an internal ATG downstream of the engineered stop.

We then tested whether *sqt*<sup>cz35</sup> mutant RNA has any activity in embryos. One-cell stage wild-type embryos were injected with synthetic capped *sqt*<sup>cz35</sup> RNA, sqt<sup>STOP</sup> or T-sqt RNA, and nuclear accumulation of β-catenin and dorsal expression of *gooseoid* (*gsc*) and *chordin* (*chd*) was examined at the onset of gastrulation (Fig. 2A-F,L,M,T). Mutant *sqt* RNA-injected embryos reached developmental landmarks at the same time as control-injected embryos (Fig. 2J,K,Q,R; data not shown), suggesting that morphogenesis or development is not generally delayed. Surprisingly, embryos injected with mutant *sqt* RNAs (sqt<sup>mut</sup>:sqt) showed expansion of nuclear β-catenin expression at the 512-cell stage, with ~16 β-catenin-positive nuclei (*n*=18 embryos), as compared with control lacZ:glo RNA-injected embryos (glo, *Xenopus globin* 3'UTR) that showed about five positive nuclei (*n*=10 embryos; Fig. 2A-D and Table 1). We detected at least 15 β-catenin-positive nuclei in more than 50% of sqt<sup>mut</sup>:sqt RNA-injected embryos, and three embryos showed more than 25 β-catenin-positive nuclei (*n*=18; Table 1 and supplementary material Table S2). The lower borders of the first tier blastoderm cells are not visible (Fig. 2A,C), consistent with yolk syncytial layer (YSL) formation at the tenth mitosis (512-cell to 1000-cell stage) (Kimmel and Law, 1985). Increased numbers of β-catenin-positive nuclei were observed both in the blastoderm (red arrows, Fig. 2A-D) and dorsal YSL of sqt<sup>mut</sup>:sqt-injected embryos (yellow arrows, Fig. 2C,D), whereas in wild-type and control-injected embryos YSL expression of β-catenin is not detected until the 1000-cell stage (supplementary material Fig. S2) (Dougan et al., 2003). Thus, injected mutant *sqt* RNA can substantially increase the dorsal accumulation of nuclear β-catenin.

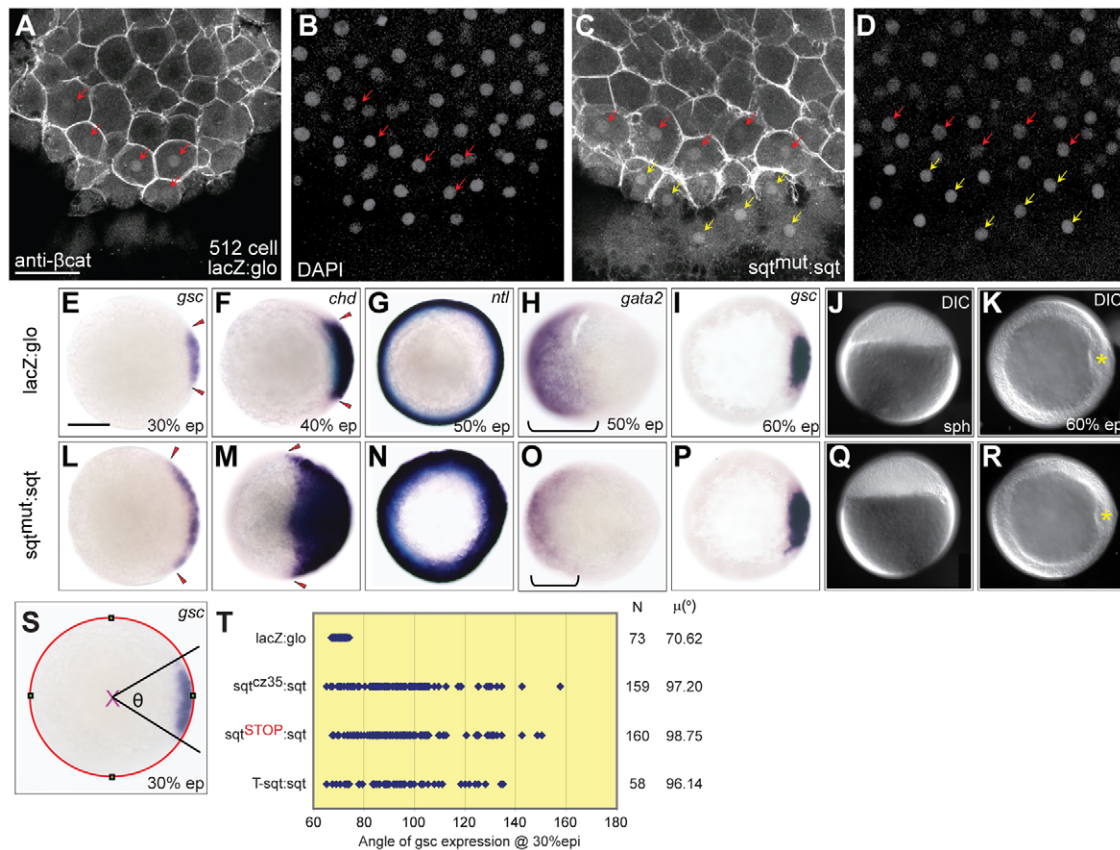


**Fig. 2. Mutant *sqt* RNAs expand the dorsal domain in early zebrafish embryos.** (A–D) Embryos injected with capped lacZ:glo mRNA show  $\beta$ -catenin in nuclei of about five cells at the 512-cell stage (A,B), in comparison to mutant *sqt* RNA-injected embryos which show  $\sim 11$   $\beta$ -catenin-positive nuclei (C,D). Red arrows indicate  $\beta$ -catenin-positive nuclei in the blastoderm, whereas yellow arrows show  $\beta$ -catenin-positive nuclei in the yolk syncytial layer (YSL). DAPI staining (B,D) shows all nuclei in blastoderm and YSL. (E–R) Normal expression of *gsc* (E), *chd* (F) and *ntl* (G) in lacZ:glo-injected embryos at 30% epiboly, 40% epiboly and 50% epiboly, respectively, as compared with expanded *gsc* (L), *chd* (M) and *ntl* (N) in mutant *sqt*:sqt UTR (*sqt*<sup>mut</sup>:sqt)-injected embryos. Expression domain of the ventral marker *gata2* (brackets in H,O) is reduced in *sqt*<sup>mut</sup>:sqt RNA-injected embryos (O), in comparison to controls (H). At 60% epiboly, *gsc* expression is similar in lacZ:glo-injected (I) and mutant *sqt*:sqt-injected (P) embryos. Embryos injected with *sqt*<sup>mut</sup>:sqt RNA reach developmental landmarks such as sphere (J,Q) and 60% epiboly (K,R) at the same time as control-injected embryos (J,K). Red arrowheads (E,F,L,M) mark the extent of *gsc* and *chd* expression; yellow asterisks (K,R) mark the shield. (S) Schematic showing measurement of *gsc* angle ( $\theta$ ). The best-fit circle is indicated in red, green squares mark x and y coordinates, and the magenta 'X' marks the center. (T) Angle of *gsc* expression in *sqt*<sup>mut</sup>:sqt RNA-injected or control lacZ-injected embryos at 30% epiboly. Each blue dot represents a single embryo. N indicates the number of injected embryos for each RNA and  $\mu(^{\circ})$  shows the mean *gsc* angles. A–D, dorsal views; E–I, K–P, R, S, animal pole views with dorsal to the right; J, Q, lateral view. Scale bars: 25  $\mu$ m in A; 100  $\mu$ m in E.

The *sqt*<sup>mut</sup>:sqt-injected embryos show expanded *gsc* expression at 30% and 40% epiboly (Fig. 2L; data not shown). Expansion of *gsc* is only observed along the margin and does not extend anteriorly. By contrast, control embryos injected with lacZ:glo RNA did not show *gsc* expansion at comparable stages (Fig. 2E; data not shown). Dorsal expansion by *sqt*<sup>mut</sup>:sqt RNAs was transient, and by 60% epiboly *gsc* expression was indistinguishable from that of control lacZ:glo RNA-injected embryos and uninjected embryos (Fig. 2I,P; data not shown). To quantify dorsal expansion, we measured the angle of *gsc* expression around the gastrula margin in injected embryos (Fig. 2S). In wild-type embryos and control lacZ:glo-injected embryos, the *gsc* angle is  $\sim 70^{\circ}$ , whereas in embryos injected with *sqt*<sup>mut</sup>:sqt RNAs the arc of *gsc* expression is much broader, resulting in angles ranging between  $70^{\circ}$  and  $150^{\circ}$ , with a mean exceeding  $95^{\circ}$  (Fig. 2T). Similarly, *chd* expression at 40% epiboly also expanded significantly (Fig. 2M). Control-injected embryos did not show expanded *gsc* or *chd*. We also

observed expanded *no tail* (*ntl*) expression around the entire margin (Fig. 2G,N), and reduced ventral gene expression of *gata2* (Fig. 2H,O) and *evel* (not shown), in comparison to control embryos.

**Table 1. Quantification of  $\beta$ -catenin-positive nuclei in injected embryos**

Injected RNA/MO	Number of $\beta$ -catenin-positive nuclei (% embryos)					Total (N)
	0-2	3-5	6-9	10-15	>15	
lacZ:glo	0	100	0	0	0	10
<i>sqt</i> <sup>mut</sup> :sqt	0	0	16.7	33.3	50	18
Con MO	0	90	10	0	0	10
<i>sqt</i> MO	100	0	0	0	0	12

Shown is the percentage of embryos that exhibit particular numbers of  $\beta$ -catenin-positive nuclei. In lacZ:glo RNA- and control MO-injected embryos, we typically detect four to five  $\beta$ -catenin-positive nuclei, and only one embryo showed six positive nuclei. By contrast, mutant *sqt* RNA-injected embryos show substantially increased numbers of  $\beta$ -catenin-positive nuclei, whereas *sqt* MO-injected embryos have reduced or no  $\beta$ -catenin-positive nuclei.

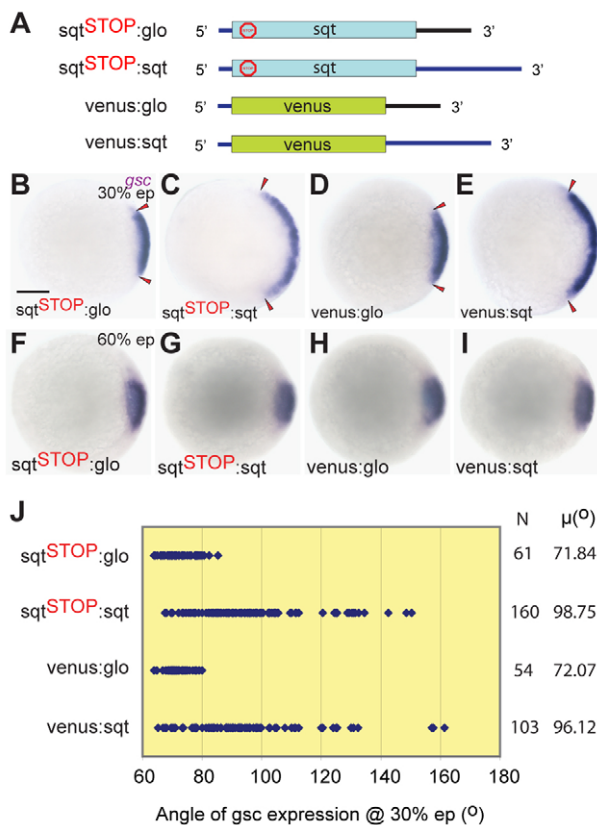


**Fig. 3. The *sqt* 3'UTR is necessary and sufficient for dorsal activity of *sqt* RNA.** (A) Schematic of constructs used to express mutant *sqt* fused with *globin* 3'UTR (black; *sqt*<sup>STOP</sup>:glo), *sqt* 3'UTR (blue; *sqt*<sup>STOP</sup>:sqt), venus (green) fused with *globin* 3'UTR (venus:glo) or *sqt* 3'UTR (venus:sqt). (B–I) Expression of *gsc* at 30% epiboly (B–E) is expanded in zebrafish embryos injected with *sqt*<sup>STOP</sup>:sqt (C) or venus:sqt (E), but not with *sqt*<sup>STOP</sup>:glo (B) or venus:glo (D). Dorsal expansion by the *sqt* 3'UTR is transient and is not detected at 60% epiboly (F–I). (J) Angle of *gsc* expansion in injected embryos at 30% epiboly. Each blue dot represents a single embryo. N indicates the number of injected embryos for each RNA and  $\mu(^{\circ})$  shows mean *gsc* angles. Scale bar: 100  $\mu$ m.

Thus, mutant *sqt* RNA that is incapable of supporting functional Sqt protein synthesis or generating the classical ligands can still expand dorsal and reduce ventral gene expression.

### Dorsal activity of *sqt* RNA is dependent on sequences in the 3'UTR

Since localization of *sqt* RNA to dorsal progenitors depends on sequences in its 3'UTR, we tested whether dorsal expansion by overexpression of *sqt* RNA also requires the 3'UTR. Embryos injected with *sqt*<sup>STOP</sup> mutant RNA fused to *sqt* 3'UTR (*sqt*<sup>STOP</sup>:sqt) were compared with those injected with mutant RNA fused with *Xenopus globin* 3'UTR (*sqt*<sup>STOP</sup>:glo; Fig. 3A). Whereas *sqt*<sup>STOP</sup>:sqt RNA injection expanded *gsc* expression at 30% epiboly (Fig. 3C), injection of *sqt*<sup>STOP</sup>:glo had no discernible effect (Fig. 3B,J), and injected embryos were indistinguishable from control or uninjected embryos. Expanded *gsc* expression in *sqt*<sup>STOP</sup>:sqt RNA-injected embryos was transient and by 60% epiboly all injected embryos were similar to uninjected (not shown) or control-injected embryos (Fig. 3F–I). Therefore, the 3'UTR is required for transient dorsal expansion by the *sqt* RNA.

We then examined whether the *sqt* 3'UTR is sufficient for dorsal expansion. Embryos were injected with RNA encoding the fluorescent protein Venus fused with either *sqt* 3'UTR (venus:sqt) or *globin* 3'UTR (venus:glo). Consistent with the evidence that the *sqt* 3'UTR is required for dorsal expansion, venus:sqt RNA-injected embryos showed transient expansion of *gsc* ranging up to 160° and with a mean of 96°. Control venus:glo-injected embryos showed a ~72° *gsc* angle (Fig. 3J), similar to uninjected embryos. Quantitative real-time RT-PCRs to detect expression of *sqt*, *dha*, *vox* and *vent* in lacZ:sqt-injected embryos showed that endogenous *sqt* and *dha* transcript levels increase transiently at sphere stages and revert to normal levels by 30% epiboly (supplementary material Fig. S3), as compared with control lacZ:glo-injected embryos. Conversely, *vox* and *vent* levels are transiently reduced initially and subsequently revert to normal (supplementary material Fig. S3). Thus, the *sqt* 3'UTR is both necessary and sufficient to transiently expand dorsal and reduce ventral gene expression.

### Activity of *sqt* 3'UTR in dorsal is independent of Sqt protein activity

Overexpressing *sqt* 3'UTR expands dorsal gene expression, but only transiently, raising the question of whether its dorsalizing activity is developmentally relevant to the embryo. To address this, we used *ichabod* (*ich*) mutant embryos, which lack all dorsal structures (Kelly et al., 2000). Embryos from homozygous *ich* mothers can be rescued by *sqt* RNA injections (Kelly et al., 2000; Gore et al., 2005). We compared the effect of *sqt* versus *globin* 3'UTR sequences on the ability of Sqt to rescue *ich* mutant embryos. Capped synthetic mRNA encoding Sqt fused to either *sqt* (*sqt*:sqt) or to *globin* (*sqt*:glo) 3'UTR was injected into *ich* embryos. In these experiments, Sqt protein would be generated from both RNAs, with the UTRs providing the only difference in activity.

Interestingly, we find that *sqt*:sqt induces a complete axis and rescues more efficiently than *sqt*:glo at comparable doses (Fig. 4A–G). Nearly 70% of *sqt*:sqt-injected embryos show rescue of dorsal structures to varying extents (15% show complete rescue and 53% partial rescue;  $n=100$  embryos; Fig. 4G) (Gore et al., 2005). By contrast, only 37% of *sqt*:glo-injected *ich* embryos show any rescue of dorsal structures. Furthermore, ~55% of *sqt*:glo-injected *ich* embryos ( $n=103$  embryos) manifest early gastrula arrest, as compared with ~30% of *sqt*:sqt injections ( $n=100$  embryos), which is likely to be due to unregulated Sqt signaling from mislocalized *sqt*:glo in contrast to localized Sqt from *sqt*:sqt. SDS-PAGE to detect Sqt protein in whole embryo lysates showed that the expression levels of Sqt from *sqt*:sqt versus *sqt*:glo are similar (Fig. 4H,I), indicating comparable translation efficiencies. These results show that the *sqt* 3'UTR confers more efficient activity to *sqt* in forming dorsal structures. Therefore, the *sqt* 3'UTR has biological activity in dorsal specification that is distinct from any activity of Sqt protein.

### Dorsal activity of *sqt* RNA requires canonical Wnt signaling but not Nodal signaling

We then tested whether dorsal expansion by *sqt* RNA requires Nodal signaling. Maternal and zygotic mutations affecting the Nodal co-receptor One-eyed pinhead (*MZoep*) are thought to cause a complete lack of Nodal signaling (Gritsman et al., 1999). In *MZoep* mutant embryos, *gsc* expression is detected at dome stages (Fig. 5A) and is not detected at mid-gastrula stages (Gritsman et al., 1999). *MZoep* embryos injected with *sqt*<sup>cz35</sup>:sqt, *sqt*<sup>STOP</sup>:sqt, lacZ:sqt and T-sqt:sqt RNA show expanded *gsc* expression at dome stages (Fig. 5A–E,P), and the *gsc* angle shows a range from 65°–

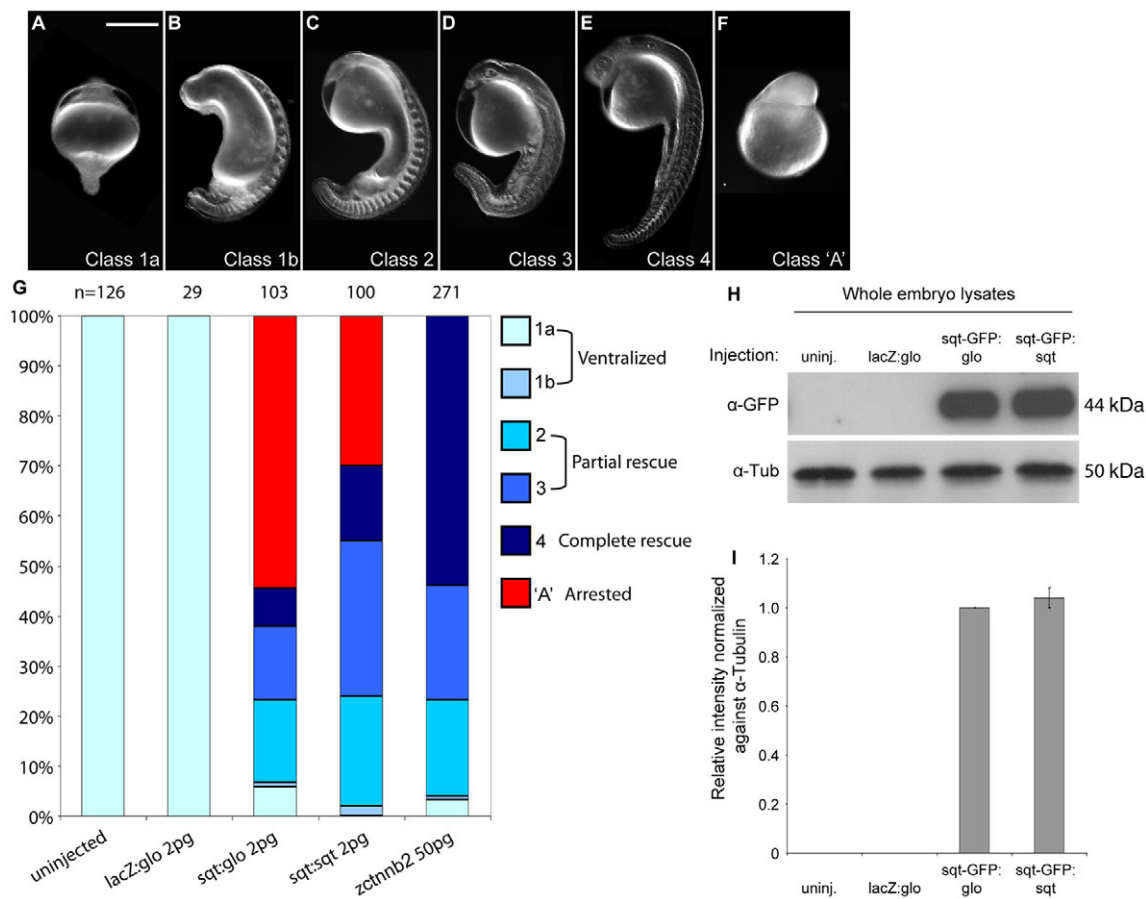


**Fig. 4. Rescue of *ichabod* embryos by Sqt is more effective with the *sqt* 3'UTR.** (A–F) Uninjected and lacZ:glo RNA-injected *ichabod* (*ich*) embryos are completely radialized (class 1a; A), whereas *sqt* or *zctnnb2* [zebrafish (*z*) *beta catenin 2*] RNA injection rescues anterior and dorsal structures to varying extents (class 1b–4; B–E), or causes early arrest (class 'A'; F). (G) Percentage embryos of each class. Injection of *sqt:sqt* and *zctnnb2* RNA is more effective in rescuing *ich* embryos than *sqt:glo*. (H) Sqt-GFP protein (44 kDa) expressed from embryos injected with *sqt-GFP:sqt* or *sqt-GFP:glo*, and lysates from uninjected embryos and lacZ:glo-injected embryos as negative controls, are shown. Tubulin (50 kDa) provides a loading control. (I) Relative intensities of Sqt-GFP bands, normalized against Tubulin, show comparable translation efficiencies of *sqt-GFP:sqt* and *sqt-GFP:glo* in whole embryo lysates. Error bars indicate s.d. between two independent experiments. Scale bar: 100  $\mu$ m.

100°, with a mean of ~88°, in comparison to control lacZ:glo-injected embryos that show *gsc* expression ranging from 63°–70°, with a mean of ~66°. Therefore, expansion of dorsal by *sqt* RNA is Oep-independent, and this function of *sqt* does not require Nodal signaling.

We then tested the requirement of maternal Wnt/ $\beta$ -catenin signaling, which is known to be essential for dorsal specification in frogs and fish (Kelly et al., 2000; Tao et al., 2005). To test whether dorsal activity of *sqt* RNA is mediated via canonical Wnt signaling, we injected mutant *sqt* RNAs into *ich* embryos and examined *gsc* expression at early gastrula. Expression of *gsc* is not expanded in *ich* embryos injected with *sqt*<sup>mut</sup>:*sqt* RNA (Fig. 5F–J,Q), in contrast to injected wild-type embryos (Fig. 5K–O,Q). Thus, expansion of dorsal by the *sqt* 3'UTR requires Wnt/ $\beta$ -catenin signaling.

#### Antisense morpholinos that target *sqt* ATG sequences block *sqt* RNA localization

The dorsal activity of maternal *sqt* RNA appears to be mediated by the 3'UTR and is independent of Sqt protein or Nodal signaling. However, these findings raise the question of how a *sqt* ATG-targeting morpholino [sqtMO1 (Gore et al., 2005; Gore

et al., 2007)] leads to loss of dorsal structures (Gore et al., 2005). *sqtMO1* spans the translational start site sequence (Feldman and Stemple, 2001) and is presumed to block Sqt protein synthesis. Indeed, co-injection of *sqtMO1* with mRNA encoding Sqt-GFP fusion protein leads to substantially reduced expression of Sqt-GFP in the blastoderm (38%, *n*=97), as compared with co-injection of Sqt-GFP with a *sqt* ATG mismatch control morpholino (ConMO, 76%, *n*=114; Fig. 6B–E). Thus, Sqt protein expression is disrupted by the ATG morpholino, but not by control morpholinos. Interestingly, we found that a substantial number of *sqtMO1*-injected embryos showed Sqt-GFP fluorescence in the yolk (~62% yolk expression, *n*=97; arrowhead in Fig. 6D), suggesting a localization defect. So, we revisited our *sqt* morpholino injection experiments (Gore et al., 2005) and tested whether *sqtMO1* also affects other functions pertaining to *sqt*, such as RNA localization and/or maintenance. To examine RNA levels, we performed RT-PCRs and found that *sqt* RNA levels are unchanged in *sqtMO1*-injected embryos at least until the 8-cell stage (supplementary material Fig. S4). Therefore, injection of the *sqt* ATG morpholino does not lead to degradation of *sqt* RNA at these stages.

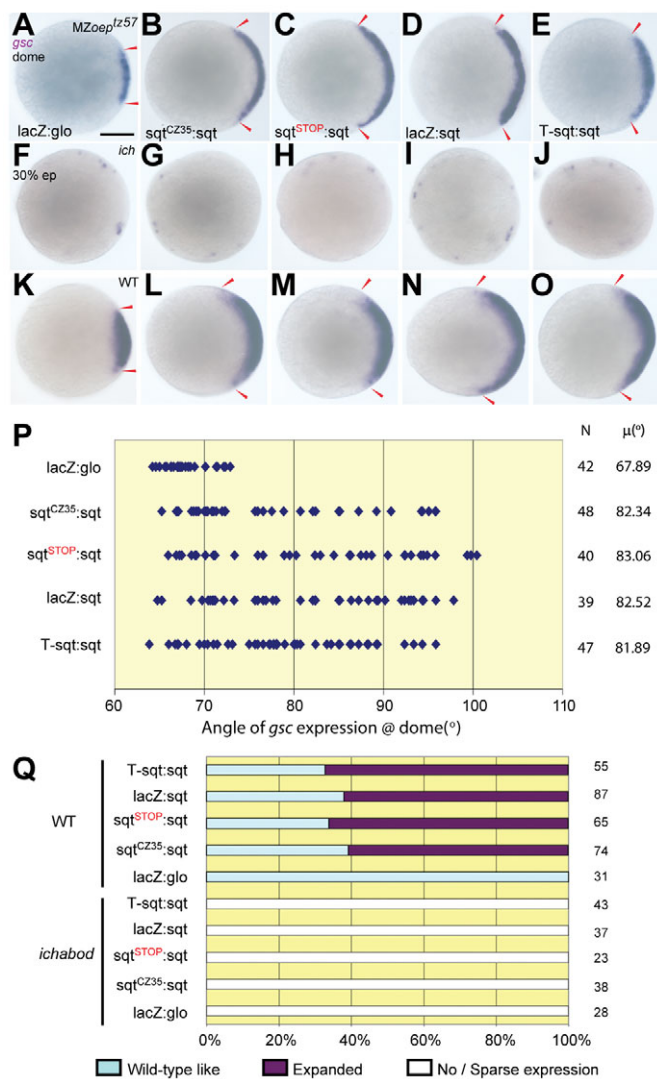


**Fig. 5. Dorsal activity of *sqt* RNA requires Wnt/β-catenin but not Nodal signaling.** (A–O) Expression of *gsc* in dome stage MZoeplz57 zebrafish embryos (A–E) shows that, compared with lacZ:glo RNA (A,F,K), injection of *sqt*<sup>CZ35</sup>:*sqt* (B,G,L), *sqt*<sup>STOP</sup>:*sqt* (C,H,M), lacZ:*sqt* (D,I,N), or T-*sqt*:*sqt* (E,J,O) RNA expands the dorsal domain (B–E), similar to that in wild-type embryos (K–O). By contrast, *ich* embryos (F–J) show no/very sparse *gsc* expression for all injected RNAs. Arrowheads (A–E,K–O) mark the extent of *gsc* expression. A–O, animal pole views; A–E, K–O, dorsal to the right. (P) The angle of *gsc* in dome stage MZoeplz57 embryos after RNA injections. Each blue dot represents a single embryo. N indicates the number of injected embryos and μ(°) shows mean *gsc* angles. (Q) Percentage embryos that manifest *gsc* expression at 30% epiboly after *sqt* RNA injections in control or *ich* mutant embryos. Scale bar: 100 μm.

To test whether *sqt*MO1 affects *sqt* RNA localization, we co-injected fluorescently labeled *sqt* RNA with either *sqt*MO1 or ConMO, and examined the embryos for localization at the 4-cell stage (Gore et al., 2005; Gilligan et al., 2011). Remarkably, *sqt*MO1 nearly abolishes *sqt* RNA localization at the 4-cell stage (90%, *n*=127), and in ~35% of the embryos the injected fluorescent *sqt* RNA was detected as aggregates in the yolk (Fig. 6G,I,J). Similarly, *sqt*MO2 (which spans exon 2/intron 2; see Fig. 6A) also affects *sqt* RNA localization (data not shown). By comparison,

ConMO and control target protector morpholinos [TP<sup>control</sup> (Giraldez et al., 2005)] do not significantly affect localization (Fig. 6F,H,J), whereas a morpholino targeting the dorsal localization element (DLE MO; see Fig. 6A) reduces *sqt* localization (Fig. 6J) (Gilligan et al., 2011). These results suggest that sequences surrounding the translational start site and splice junctions are also required for *sqt* RNA localization. Therefore, in addition to disrupting the translation/splicing of *sqt* RNA, the *sqt* morpholinos also unexpectedly affect *sqt* RNA localization.

### Disruption of *sqt* RNA localization leads to ectopic dorsal expansion

We find that blocking the translational start site disrupts *sqt* RNA localization (Fig. 6). However, *sqt* RNA localization is also dependent on sequences in the 3'UTR (Gore et al., 2005; Gilligan et al., 2011), and dorsal expansion also requires the 3'UTR. We therefore tested whether dorsal expansion by the 3'UTR depends on *sqt* RNA localization. We injected DLE MO, which disrupts *sqt* RNA localization (Gilligan et al., 2011). Morpholinos targeting a different region of the *sqt* 3'UTR (TP<sup>control</sup> MO) and miR430 target protector morpholinos [TP<sup>miR430</sup> MO (Giraldez et al., 2005)] were used as controls. Embryos injected with the DLE MO showed lateral expansion of dorsal *gsc* expression even at low doses (2 ng; Fig. 7B,E), similar to embryos injected with non-coding *sqt* RNA (see Fig. 2F and Fig. 3C,E). At higher doses (10 ng), *gsc* expression extended further towards the animal pole (Fig. 7C,E) or even covered the entire blastoderm (Fig. 7D,E). By contrast, TP<sup>control</sup> MO-injected and TP<sup>miR430</sup> MO-injected embryos did not manifest *gsc* expansion at 2 ng doses, and only a few TP<sup>miR430</sup> MO-injected embryos showed mild expansion of *gsc* at 10 ng (Fig. 7E). These experiments show that blocking the dorsal localization element in endogenous *sqt* RNA with DLE MO leads to expanded or ectopic *gsc* expression. Thus, dorsal expansion by *sqt* RNA is not dependent on the DLE in the *sqt* 3'UTR.

We also examined the expression of early dorsal markers in *sqt* ATG morphant embryos. Injection of *sqt* morpholinos into eggs to target maternal *sqt* RNA prior to the formation of aggregates in the yolk upon egg activation (Gore and Sampath, 2002) causes loss of dorsal specification. We find that *gsc* expression is not detected in these embryos, consistent with the loss of dorsal structures (Fig. 7G). This is in contrast to MZ*sqt* and MZ*oeplz57* mutant embryos, in which early *gsc* expression is detected at comparable stages (Fig. 7H,I and Fig. 5A). Furthermore, β-catenin fails to accumulate in dorsal nuclei of *sqt*MO1-injected embryos, in contrast to ConMO-injected embryos (Fig. 7N–Q, Table 1 and supplementary material Table S2). Ventral markers such as *gata2* are concomitantly expanded in *sqt*MO1-injected embryos (Fig. 7J–M). Therefore, the sequences spanning the translational start site in *sqt* RNA are required for localization, and disruption of endogenous *sqt* function by *sqt*MO1 leads to loss of dorsal gene expression, probably by blocking both maternal *sqt* RNA localization and translation. These results also show that maternal *sqt* RNA functions prior to nuclear β-catenin accumulation.

### The *sqt* 3'UTR rescues anterior and dorsal structures in *sqt* morphant embryos

We then tested whether the *sqt* 3'UTR is capable of restoring early dorsal *gsc* expression in *sqt* morphant embryos. In comparison to control morpholino-injected embryos (Fig. 8A), MZ*sqt* and MZ*oeplz57* embryos (Fig. 7H,I and Fig. 5A), injection of the *sqt* morpholinos into eggs results in embryos with severe dorsal deficiencies (Gore et al., 2005; Gore et al., 2007) and loss

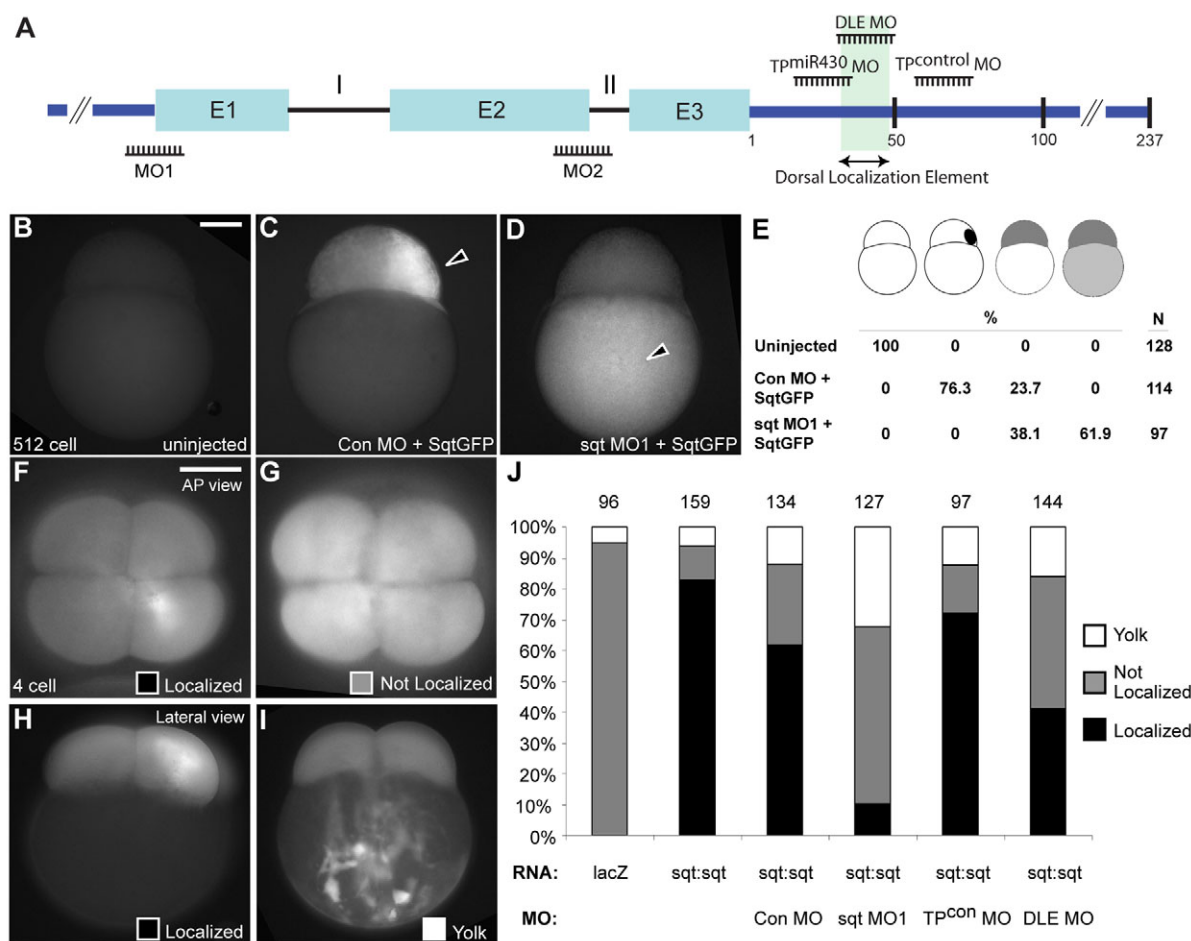


**Fig. 6. Morpholinos targeting the *sqt* ATG disrupt *sqt* RNA localization.** (A) The zebrafish *sqt* genomic locus (not to scale) indicating positions of the *sqt* ATG morpholino (MO1), *sqt* intron 2 morpholino (MO2), *sqt* DLE morpholino (DLE MO), *sqt* miR430 target protector morpholino (TP<sup>miR430</sup> MO), and target protector control morpholino (TP<sup>control</sup> MO). Introns (I and II), exons (E1, E2 and E3; cyan boxes) and UTR (dark blue line) are indicated. The dorsal localization element is highlighted in green. (B–D) Embryos injected with *sqt*-GFP RNA show asymmetric expression of Sq-GFP fluorescent protein in the blastoderm of 512-cell stage embryos (C), in comparison to uninjected embryos (B) and embryos co-injected with *sqt*MO1 and *sqt*-GFP that show Sq-GFP fluorescence in the yolk (D). (E) Numbers (N) and percentage of embryos showing no expression, expression of Sq-GFP in the blastoderm, yolk, or both. (F–I) Localization of injected fluorescent control *lacZ* or *sqt*:*sqt* RNA in 4-cell stage embryos co-injected with control morpholinos, *sqt*MO1, TP<sup>control</sup> MO or DLE MO. (J) Percentage and number of embryos (top) showing *sqt* RNA localized (F,H), not localized (G), or as aggregates in the yolk (I). Lateral views at 512-cell stage (B–D) or 4-cell stage (H,I), or animal pole views at 4-cell stage (F,G). Scale bars: 100 μm.

of *gsc* expression (Fig. 8C). Co-injection of *lacZ*:*sqt* or *sqt*<sup>STOP</sup>:*sqt* RNA with *sqt*MO1 or *sqt*MO2 rescued early *gsc* expression in *sqt* morphant embryos (Fig. 8E and supplementary material Fig. S5), whereas co-injection of *lacZ*:*glo* RNA with *sqt*MOs did not restore *gsc* expression (supplementary material Fig. S5). At prim-5 stages, *sqt* morpholino-injected embryos manifest loss of anterior and dorsal structures, whereas co-injection of the *sqt*MOs with *sqt*<sup>mut</sup> RNA or *lacZ*:*sqt* RNA produces phenotypes that are strikingly similar to that of MZ*sqt*<sup>cz35</sup> mutant embryos (Fig. 8D,F,H,I). The *sqt* morpholinos prevent endogenous Sqt protein translation and endogenous *sqt* RNA localization, but cannot target *lacZ*:*sqt*. Therefore, the rescue by the *sqt* 3'UTR sequences is very significant. Thus, *sqt* RNA, and specifically the *sqt* 3'UTR, is sufficient to initiate dorsal gene expression in early embryos. These findings indicate that the biological activity of maternal *sqt* RNA in dorsal specification is likely to reside within its 3'UTR.

## DISCUSSION

Asymmetric localization of *sqt* RNA in presumptive dorsal cells shows that dorsoventral asymmetry in the blastoderm is established prior to zygotic transcription, during cleavage stages. Based upon cell ablations and antisense morpholino injections, we proposed that asymmetrically localized *sqt* RNA and associated factors specify dorsal identity (Gore et al., 2005). However, studies using the insertion mutants *sqt*<sup>cz35</sup> and *sqt*<sup>hi975</sup> suggested that early specification of the dorsoventral axis might not require the activity of maternal Sqt (Aoki et al., 2002; Bennett et al., 2007; Pei et al., 2007). Therefore, the function of maternal *sqt* was unclear. We find that *sqt* RNA has functions that are independent of Sqt protein in dorsal initiation. Furthermore, we show that the *sqt*<sup>cz35</sup> and *sqt*<sup>hi975</sup> insertion alleles are not maternal transcript nulls: *sqt*<sup>cz35</sup> RNA is expressed in MZ*sqt* at similar levels to *sqt* in wild-type embryos at early stages and also localizes to two cells in 4- and 8-cell stage embryos. We observed a reduction in *sqt* RNA levels during

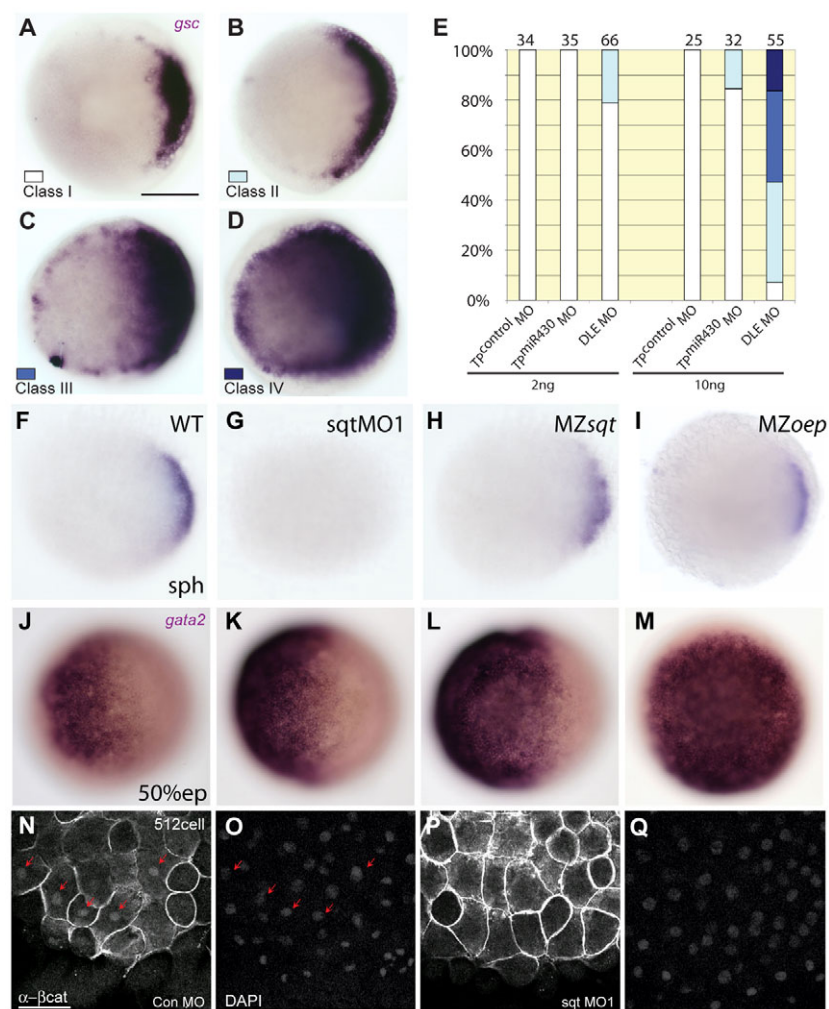


**Fig. 7. The *sqt* DLE MO and ATG MO differentially affect dorsal gene expression.** (A–E) *gsc* expression expands upon injection of the DLE MO even at low doses, in comparison to injections of TpmiR430 MO or Tpcontrol MO. (E) The percentage and number of embryos and the extent of *gsc* expression (classes I–IV, A–D) in injected embryos at sphere stages. (F–I) Expression of *gsc* is abolished in *sqt*MO1-injected embryos at the sphere stage (G), in comparison to control wild-type (F), MZ*sqt* (H) or MZ*oepl* (I) embryos. (J–M) Expression of the ventral marker gene *gata2* is expanded to varying extents in *sqt*MO1-injected embryos (K–M), in comparison to control embryos (J). (N–Q) Nuclear  $\beta$ -catenin (N,P) in dorsal cells is not detected in *sqt*MO1-injected embryos at the 512-cell stage (P,Q), in contrast to ConMO-injected embryos (arrows, N,O). DAPI staining (O,Q) shows the presence of nuclei. (A–D,F–M) Animal pole views; (N–Q) dorsal views. Scale bars: 100  $\mu$ m in A; 25  $\mu$ m in N.

gastrulation, consistent with a previous report of reduced *sqt* mutant transcripts in late blastula embryos (Bennett et al., 2007). However, Bennett et al. (Bennett et al., 2007) also stated that MZ*sqt*<sup>cz35</sup> embryos at the 8-cell stage contain no detectable *sqt* RNA using *sqt*-specific RT-PCR primers, and Pei et al. (Pei et al., 2007) reported that *sqt* RNA is reduced or absent in MZ*sqt*<sup>hi975</sup> embryos based on RT-PCR using oligo(dT)-primed cDNA. By RNA sequencing and RT-PCR, we find that maternally deposited *sqt* RNA is non-polyadenylated and unspliced, and that *sqt* mRNA is detected during cleavage stages (supplementary material Fig. S1A,B) (Gore et al., 2007), providing an explanation for the Pei et al. (Pei et al., 2007) observation. However, our findings differ from the lack of maternal *sqt* RNA reported by Bennett et al. (Bennett et al., 2007), which we detect in early MZ*sqt* embryos by RT-PCR, quantitative PCR and whole-mount in situ hybridization.

We previously reported that injection of *sqt* splice-blocking morpholinos into wild-type eggs leads to aberrantly spliced *sqt* RNA (Gore et al., 2007). The presence of pre-mRNAs has been reported in oocytes in other metazoans as well (Hachet and Ephrussi, 2004). In *Xenopus* eggs, many maternal pre-mRNAs are also known to be non-polyadenylated or have very short poly(A) tails, which presumably prevent precocious protein translation (Sagata et al., 1980; McGrew et al., 1989; Paris and Philippe, 1990; Varnum and Wormington, 1990). Our findings are also consistent with the recent genome-wide transcriptome analysis in zebrafish by Aanes et al. (Aanes et al., 2011), who showed by RNA

sequencing that a large cohort of maternal transcripts in zebrafish eggs are non-polyadenylated, and become polyadenylated during early embryogenesis (Aanes et al., 2011). Thus, the *sqt* insertion alleles are not maternal transcript nulls and not bona fide functional null alleles.

Mutant *sqt* RNA can expand dorsal gene expression in wild-type embryos, with a concomitant reduction in ventral gene expression. The transient *gsc* expansion by *sqt*<sup>mut</sup>:*sqt* RNAs and the *sqt* 3'UTR is unlikely to be due to a morphological delay as the embryos are not generally delayed. Moreover, the *gsc* expansion is restricted to the gastrula margin and does not extend anteriorly, in contrast to the broad *gsc* expression domain reported in early embryos (Schulte-Merker et al., 1994). We also observed expansion of *chd* and substantially increased numbers of  $\beta$ -catenin-positive nuclei in embryos injected with non-coding *sqt* RNA. Furthermore, *dha* and endogenous *sqt* transcript levels transiently increase, with a concomitant reduction in *vox* and *vent* transcripts, providing the basis for the transient increase in *chd*, *gsc* and *ntl* and reduction in ventral expression of *gata2* (Hammerschmidt et al., 1996; Erter et al., 1998; Rebagliati et al., 1998; Yamanaka et al., 1998; Imai et al., 2001; Gilardelli et al., 2004). Thus, *sqt* RNA, and specifically the *sqt* 3'UTR, can nucleate a complex of factors that are sufficient to expand dorsal gene expression. We also find that mutant/non-coding *sqt* RNA injections into *sqt* morphants can phenocopy MZ*sqt* mutant embryos. Taken together, these findings suggest that it is the

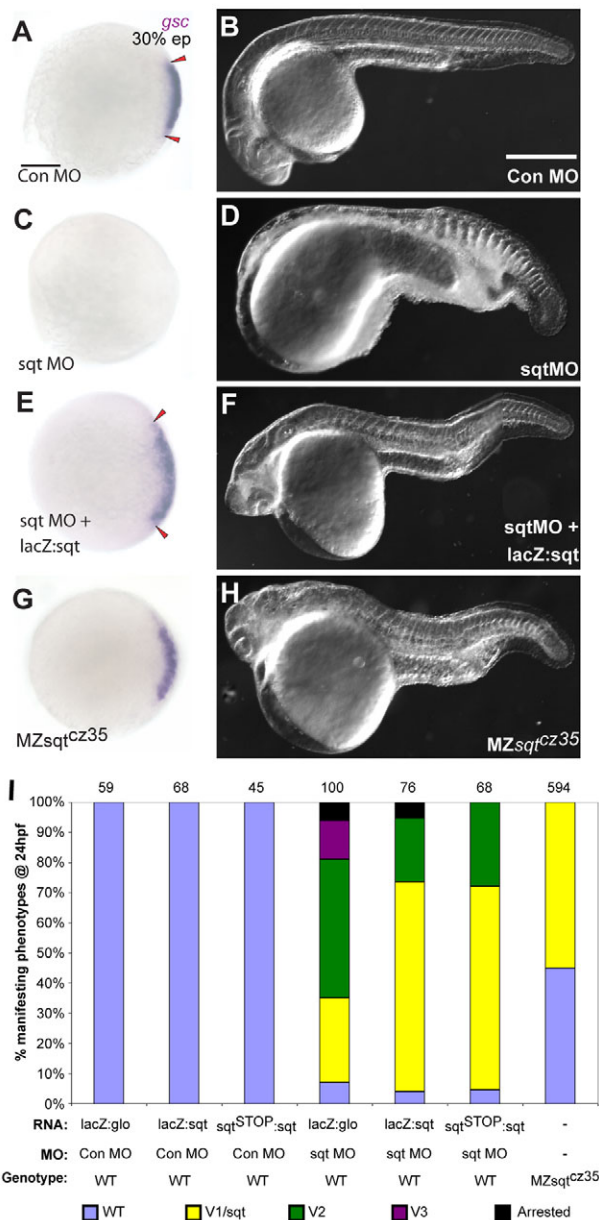


**Fig. 8. Loss of dorsal specification due to *sqt* morpholinos is rescued by the *sqt* 3'UTR.** (A-H) Early *gsc* expression is not detected in *sqt*MO-injected (C), in contrast to ConMO-injected (A), zebrafish embryos. Expression of *gsc* is rescued in *sqt* morphants by co-injection of *lacZ:sqt* (E), but not with *lacZ:glo* (see supplementary material Fig. S4). Embryos co-injected with *sqt*MO and *lacZ:sqt* (F,I) or *sqt*MO and *sqt*<sup>STOP</sup>:*sqt* (I) are rescued partially and are similar to MZ*sqt*<sup>c235</sup> mutant embryos (H). Images in F,H were acquired in different focal planes for the rostral and caudal regions of the embryo and subsequently assembled. (A,C,E,G) 30% epiboly, animal pole views with dorsal to the right; (B,D,F,H) prim-5 stage. Arrowheads (A,E) mark the extent of *gsc* expression. (I) Extent of rescue of *sqt*MO-injected embryos by co-injection of *lacZ:sqt* or *sqt*<sup>STOP</sup>:*sqt*, versus control *lacZ:glo* RNA. Scale bars: 100  $\mu$ m.

activity of the mutant *sqt* transcripts in the maternal *sqt* insertion mutants that leads to initial dorsal expression in mutant embryos, and MZ*sqt* mutants do not exhibit the severe loss of dorsal identity manifested by *sqt* morphants in which maternal *sqt* RNA localization and activity are both disrupted.

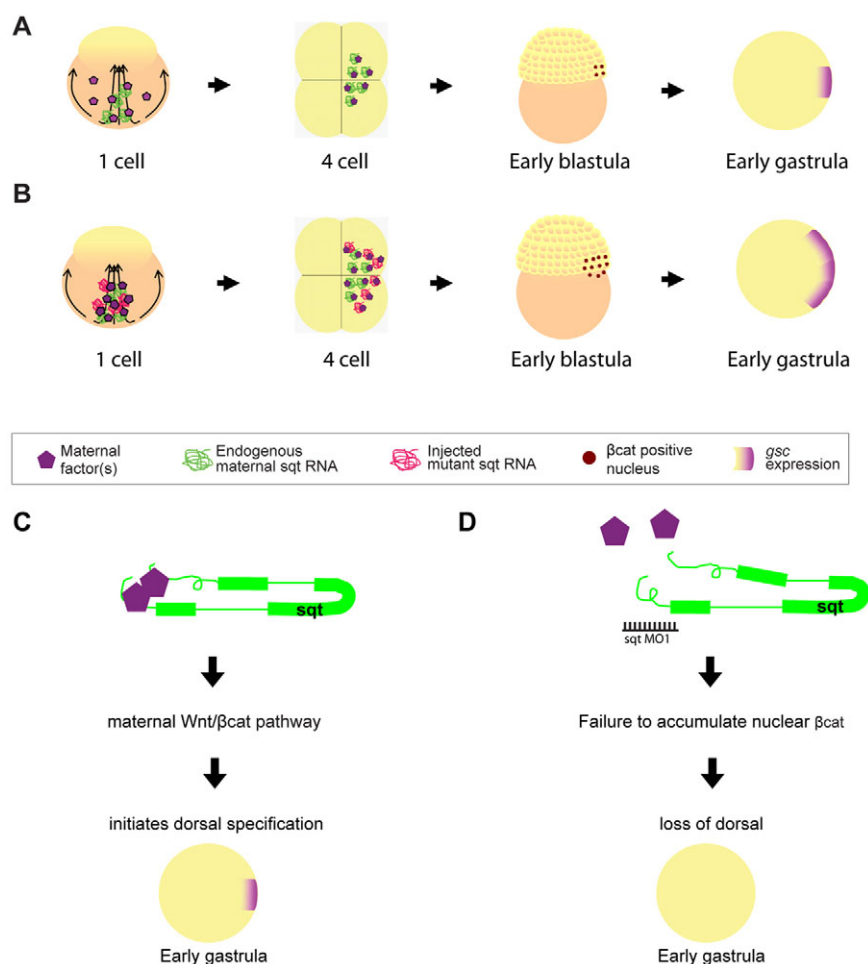
Interestingly, we never detected any ectopic sites of *gsc* or *chd* in the mutant *sqt* RNA-injected embryos, unlike those injected with wild-type *sqt* RNA (Erter et al., 1998; Rebagliati et al., 1998). Thus, although mutant *sqt* RNAs and the *sqt* 3'UTR can expand the endogenous dorsal domain, these *sqt* sequences do not induce dorsal at ectopic locations, presumably because these RNAs harbor the dorsal localization element. By contrast, injection of *sqt* DLE MO to target endogenous *sqt* RNA leads to ectopic *gsc* expression, probably owing to mislocalization and misexpression of endogenous Sqt.

Mutant *sqt* RNAs transiently expand the dorsal domain in wild-type embryos, but this expansion is not sustained, and by mid-gastrula stages the embryos appear to have regulated dorsal gene expression levels back to that observed in control embryos. This transient expansion is consistent with the normal *gsc* expression observed at 70% epiboly by Bennett et al. (Bennett et al., 2007) in T-*sqt*-injected embryos. Similar changes in early patterning with no overt later consequences have also been observed in other contexts/organisms. For example, extra copies of *bicoid*<sup>+</sup> in *Drosophila* lead to transient oversized head regions in embryos, which develop into apparently normal adults (Berleth et al., 1988).

Dorsal *gsc* expression is also expanded in MZ*oep* embryos, which are presumed to lack all Nodal signaling (Gritsman et al., 1999). However, the expansion is not sustained. Initiation of dorsal *gsc* expression and its subsequent loss has been reported previously in *cyc*; *sqt* compound mutant embryos (Dogan et al., 2003). Thus, maintenance of *gsc* expression during gastrulation requires Nodal signaling. Although *sqt* RNA can initiate and expand dorsal gene expression independently of Sqt protein or *Oep*-dependent Nodal signaling, the sustained expression of dorsal genes requires the signaling functions of Sqt mediated via *Oep*.

So how does *sqt* RNA function to initiate and expand dorsal? This is likely to be a non-coding function of *sqt*, as the *sqt* 3'UTR even when fused to heterologous reporter genes (*lacZ* or *venus*) can expand dorsal gene expression in wild-type embryos and rescues early dorsal gene expression in *sqt* morphants. Furthermore, coding *sqt* sequences fused to the *sqt* 3'UTR rescue *ich* embryos more efficiently than *sqt* fused to *globin* UTR sequences, demonstrating that the activity of the *sqt* 3'UTR is distinct from the Sqt coding sequences. Taken together, these findings suggest that *sqt* RNA, and specifically the *sqt* 3'UTR, functions in dorsal specification. Our current evidence is based upon overexpression and knockdown strategies, which have their limitations (Robu et al., 2007; Eisen and Smith, 2008). Although it is imperative to determine whether a *sqt* mutant that lacks maternal *sqt* RNA expression also lacks dorsal identity, such a mutant is not yet available despite our attempts using zinc-finger nuclease (ZFN) (Doyon et al., 2008; Meng et al., 2008) technology.

The *sqt* 3'UTR harbors microRNA (miRNA) target sites (Giraldez et al., 2006; Choi et al., 2007), raising the possibility that dorsalization by the *sqt* 3'UTR might be mediated via miRNAs. However, this seems unlikely because *sqt* 3'UTR with mutations in target site sequences of three predicted miRNAs still expands the dorsal domain, as does *sqt* RNA injection into MZ*dicer* embryos (supplementary material Fig. S6). Although it remains possible that there are other unidentified *dicer*-independent small RNA targets in the *sqt* 3'UTR, our experiments show that the *sqt* 3'UTR functions independently of the miRNAs tested and of *dicer*. Rather, we surmise that *sqt* RNA might translocate some factor(s)/protein(s) that bind to the UTRs to the future dorsal side. In *Drosophila*, *oskar* RNA has



functions that are independent of Oskar protein in early oogenesis (Jenny et al., 2006). Similarly, *Xenopus veg-T* RNA has a scaffolding function that is independent of the later functions of Veg-T protein in germ layer specification (Zhang and King, 1996; Kloc et al., 2005). Since *sqt* RNA is normally present in limiting amounts in early embryos (Rebagliati et al., 1998; Gore et al., 2005), even small increases in the amount of *sqt* 3'UTR could lead to an amplified effect of any UTR-bound factors (see model in Fig. 9) in the future embryonic dorsal side. These factor(s) might function via the canonical Wnt/ $\beta$ -catenin pathway, as the *sqt* 3'UTR by itself is unable to expand the dorsal domain in the context of *ich* embryos, which are deficient in  $\beta$ -catenin signaling. It is conceivable that the factor(s) binding to the *sqt* 3'UTR are components of the Wnt/ $\beta$ -catenin pathway.

In *Xenopus*, RNA encoding Xwnt11, which is required for dorsal specification and functions via  $\beta$ -catenin (Tao et al., 2005), is localized to dorsal vegetal cells of early embryos. The factors that bind and localize Xwnt11 RNA are not known. In zebrafish, embryos from *ich* mutant mothers show that maternal  $\beta$ -catenin function is required for dorsal specification, and maternal *wnt8a* RNA is likely to activate Wnt/ $\beta$ -catenin signaling (Lu et al., 2011). Asymmetric localization of *sqt* RNA in the blastoderm by the 4-cell stage precedes dorsal accumulation of nuclear  $\beta$ -catenin at the 128-cell stage (Dougan et al., 2003; Gore et al., 2005).

The *sqt* 5'UTR and 3'UTR both affect *sqt* RNA localization, but somewhat differently. Whereas the *sqt* ATG morpholino results in *sqt* RNA being mislocalized diffusely or stuck in the yolk as aggregates, the DLE MO causes *sqt* RNA to be mislocalized diffusely in the blastoderm. The phenotypes caused by the morpholinos targeting these two regions are also distinct in that the ATG morpholino causes loss of nuclear  $\beta$ -catenin and loss of *gsc* expression, whereas the 3'UTR DLE MO causes mislocalized and ectopic *gsc*, probably owing to mislocalized endogenous Sqt in the blastoderm. This suggests that the *sqt* 5'UTR and 3'UTR sequences might function in distinct steps of *sqt* RNA localization and activity. Moreover, our finding that the *sqt* ATG morpholino disrupts both *sqt* RNA localization and translation suggests that the *sqt* 5'UTR and 3'UTR sequences might interact with each other, perhaps via binding of a protein complex, to regulate *sqt* RNA localization (see model in Fig. 9). The *sqt* morpholinos cause loss of dorsal nuclear  $\beta$ -catenin and *gsc* expression, which might underlie the severe loss of dorsal structures in the morphants. Our results suggest that localized maternal *sqt* RNA functions prior to the accumulation of nuclear  $\beta$ -catenin, and raise the possibility that *sqt* RNA acts as a scaffold to bind and deliver/sequester maternal factors, which are likely to be intracellular component(s) of the Wnt pathway, to future dorsal. Our findings identify novel functions for the Nodal genes and suggest a new role for non-coding RNAs in the control of axis specification.

## Acknowledgements

We thank members of the K.S. laboratory, the Singapore fish community, Tom Carney, Bill Chia, Steve Cohen, Ray Dunn, Aniket Gore, Masahiko Hibi, Greg Jedd, Mithilesh Mishra and Mohan Balasubramanian for discussions and suggestions; Shingo Maegawa and Eric Weinberg for *ich* fish; and the Temasek Life Sciences Laboratory sequencing and fish facilities.

## Funding

S.L. was supported by a pre-doctoral fellowship from the Singapore Millennium Foundation and Temasek Life Sciences Laboratory; S.M. is supported by the Genome Institute of Singapore; work in the laboratory of K.S. is supported by Temasek Life Sciences Laboratory.

## Competing interests statement

The authors declare no competing financial interests.

## Supplementary material

Supplementary material available online at  
<http://dev.biologists.org/lookup/suppl/doi:10.1242/dev.077081/-DC1>

## References

- Aanes, H., Winata, C. L., Lin, C. H., Chen, J. P., Srinivasan, K. G., Lee, S. G., Lim, A. Y., Hajan, H. S., Collas, P., Bourque, G. et al. (2011). Zebrafish mRNA sequencing deciphers novelties in transcriptome dynamics during maternal to zygotic transition. *Genome Res.* **21**, 1328-1338.
- Abrams, E. W. and Mullins, M. C. (2009). Early zebrafish development: it's in the maternal genes. *Curr. Opin. Genet. Dev.* **19**, 396-403.
- Amsterdam, A., Nissen, R. M., Sun, Z., Swindell, E. C., Farrington, S. and Hopkins, N. (2004). Identification of 315 genes essential for early zebrafish development. *Proc. Natl. Acad. Sci. USA* **101**, 12792-12797.
- Aoki, T. O., Mathieu, J., Saint-Etienne, L., Rebagliati, M. R., Peyrieras, N. and Rosa, F. M. (2002). Regulation of nodal signalling and mesendoderm formation by TARAM-A, a TGFbeta-related type I receptor. *Dev. Biol.* **241**, 273-288.
- Bellipanni, G., Varga, M., Maegawa, S., Imai, Y., Kelly, C., Myers, A. P., Chu, F., Talbot, W. S. and Weinberg, E. S. (2006). Essential and opposing roles of zebrafish beta-catenins in the formation of dorsal axial structures and neurectoderm. *Development* **133**, 1299-1309.
- Bennett, J. T., Stickney, H. L., Choi, W. Y., Ciruna, B., Talbot, W. S. and Schier, A. F. (2007). Maternal nodal and zebrafish embryogenesis. *Nature* **450**, E1-E2.
- Berleth, T., Burri, M., Thoma, G., Bopp, D., Richstein, S., Frigerio, G., Noll, M. and Nusslein-Volhard, C. (1988). The role of localization of bicoid RNA in organizing the anterior pattern of the *Drosophila* embryo. *EMBO J.* **7**, 1749-1756.
- Choi, W. Y., Giraldez, A. J. and Schier, A. F. (2007). Target protectors reveal dampening and balancing of Nodal agonist and antagonist by miR-430. *Science* **318**, 271-274.
- Cuykendall, T. N. and Houston, D. W. (2009). Vegetally localized *Xenopus* trim36 regulates cortical rotation and dorsal axis formation. *Development* **136**, 3057-3065.
- Dougan, S. T., Warga, R. M., Kane, D. A., Schier, A. F. and Talbot, W. S. (2003). The role of the zebrafish nodal-related genes *squint* and *cyclops* in patterning of mesendoderm. *Development* **130**, 1837-1851.
- Doyon, Y., McCammon, J. M., Miller, J. C., Faraji, F., Ngo, C., Katibah, G. E., Amora, R., Hocking, T. D., Zhang, L., Rebar, E. J. et al. (2008). Heritable targeted gene disruption in zebrafish using designed zinc-finger nucleases. *Nat. Biotechnol.* **26**, 702-708.
- Eisen, J. S. and Smith, J. C. (2008). Controlling morpholino experiments: don't stop making antisense. *Development* **135**, 1735-1743.
- Erter, C. E., Solnica-Krezel, L. and Wright, C. V. (1998). Zebrafish nodal-related 2 encodes an early mesendodermal inducer signaling from the extraembryonic yolk syncytial layer. *Dev. Biol.* **204**, 361-372.
- Feldman, B. and Stemple, D. L. (2001). Morpholino phenocopies of *sqt*, *oep*, and *ntl* mutations. *Genesis* **30**, 175-177.
- Feldman, B., Gates, M. A., Egan, E. S., Dougan, S. T., Rennebeck, G., Sirotkin, H. I., Schier, A. F. and Talbot, W. S. (1998). Zebrafish organizer development and germ-layer formation require nodal-related signals. *Nature* **395**, 181-185.
- Gilardelli, C. N., Pozzoli, O., Sordino, P., Matassi, G. and Cotelli, F. (2004). Functional and hierarchical interactions among zebrafish *vox/vent* homeobox genes. *Dev. Dyn.* **230**, 494-508.
- Gilligan, P. C., Kumari, P., Lim, S., Cheong, A., Chang, A. and Sampath, K. (2011). Conservation defines functional motifs in the *squint*/nodal-related 1 RNA dorsal localization element. *Nucleic Acids Res.* **39**, 3340-3349.
- Giraldez, A. J., Cinalli, R. M., Glasner, M. E., Enright, A. J., Thomson, J. M., Baskerville, S., Hammond, S. M., Bartel, D. P. and Schier, A. F. (2005). MicroRNAs regulate brain morphogenesis in zebrafish. *Science* **308**, 833-838.
- Giraldez, A. J., Mishima, Y., Rihel, J., Grocock, R. J., Van Dongen, S., Inoue, K., Enright, A. J. and Schier, A. F. (2006). Zebrafish miR-430 promotes deadenylation and clearance of maternal mRNAs. *Science* **312**, 75-79.
- Gore, A. V. and Sampath, K. (2002). Localization of transcripts of the zebrafish morphogen *Squint* is dependent on egg activation and the microtubule cytoskeleton. *Mech. Dev.* **112**, 153-156.
- Gore, A. V., Maegawa, S., Cheong, A., Gilligan, P. C., Weinberg, E. S. and Sampath, K. (2005). The zebrafish dorsal axis is apparent at the four-cell stage. *Nature* **438**, 1030-1035.
- Gore, A. V., Cheong, A., Gilligan, P. C. and Sampath, K. (2007). Gore et al. reply to J. T. Bennett et al. *Nature* **450**, E2-E4.
- Gritsman, K., Zhang, J., Cheng, S., Heckscher, E., Talbot, W. S. and Schier, A. F. (1999). The EGF-CFC protein one-eyed pinhead is essential for nodal signaling. *Cell* **97**, 121-132.
- Grunert, S. and St Johnston, D. (1996). RNA localization and the development of asymmetry during *Drosophila* oogenesis. *Curr. Opin. Genet. Dev.* **6**, 395-402.
- Hachet, O. and Ephrussi, A. (2004). Splicing of oskar RNA in the nucleus is coupled to its cytoplasmic localization. *Nature* **428**, 959-963.
- Hammerschmidt, M., Serbedzija, G. N. and McMahon, A. P. (1996). Genetic analysis of dorsoventral pattern formation in the zebrafish: requirement of a BMP-like ventralizing activity and its dorsal repressor. *Genes Dev.* **10**, 2452-2461.
- Heasman, J. (2006). Maternal determinants of embryonic cell fate. *Semin. Cell Dev. Biol.* **17**, 93-98.
- Heasman, J., Crawford, A., Goldstone, K., Garner-Hamrick, P., Gumbiner, B., McCrea, P., Kintner, C., Noro, C. Y. and Wylie, C. (1994). Overexpression of cadherins and underexpression of beta-catenin inhibit dorsal mesoderm induction in early *Xenopus* embryos. *Cell* **79**, 791-803.
- Heasman, J., Kofron, M. and Wylie, C. (2000). Beta-catenin signaling activity dissected in the early *Xenopus* embryo: a novel antisense approach. *Dev. Biol.* **222**, 124-134.
- Heisenberg, C. P. and Nusslein-Volhard, C. (1997). The function of *silberblick* in the positioning of the eye anlage in the zebrafish embryo. *Dev. Biol.* **184**, 85-94.
- Imai, Y., Gates, M. A., Melby, A. E., Kimelman, D., Schier, A. F. and Talbot, W. S. (2001). The homeobox genes *vox* and *vent* are redundant repressors of dorsal fates in zebrafish. *Development* **128**, 2407-2420.
- Jenny, A., Hachet, O., Zavorsky, P., Cyrklaff, A., Weston, M. D., Johnston, D. S., Erdelyi, M. and Ephrussi, A. (2006). A translation-independent role of oskar RNA in early *Drosophila* oogenesis. *Development* **133**, 2827-2833.
- Jesuthasan, S. and Strahle, U. (1997). Dynamic microtubules and specification of the zebrafish embryonic axis. *Curr. Biol.* **7**, 31-42.
- Kelly, C., Chin, A. J., Leatherman, J. L., Kozlowski, D. J. and Weinberg, E. S. (2000). Maternally controlled (beta)-catenin-mediated signaling is required for organizer formation in the zebrafish. *Development* **127**, 3899-3911.
- Kimmel, C. B. and Law, R. D. (1985). Cell lineage of zebrafish blastomeres. II. Formation of the yolk syncytial layer. *Dev. Biol.* **108**, 86-93.
- Kloc, M., Wilk, K., Vargas, D., Shirato, Y., Bilinski, S. and Etkin, L. D. (2005). Potential structural role of non-coding and coding RNAs in the organization of the cytoskeleton at the vegetal cortex of *Xenopus* oocytes. *Development* **132**, 3445-3457.
- Kofron, M., Klein, P., Zhang, F., Houston, D. W., Schaible, K., Wylie, C. and Heasman, J. (2001). The role of maternal axin in patterning the *Xenopus* embryo. *Dev. Biol.* **237**, 183-201.
- Lu, F. I., Thisse, C. and Thisse, B. (2011). Identification and mechanism of regulation of the zebrafish dorsal determinant. *Proc. Natl. Acad. Sci. USA* **108**, 15876-15880.
- McGrew, L. L., Dworkin-Rastl, E., Dworkin, M. B. and Richter, J. D. (1989). Poly(A) elongation during *Xenopus* oocyte maturation is required for translational recruitment and is mediated by a short sequence element. *Genes Dev.* **3**, 803-815.
- Meng, X., Noyes, M. B., Zhu, L. J., Lawson, N. D. and Wolfe, S. A. (2008). Targeted gene inactivation in zebrafish using engineered zinc-finger nucleases. *Nat. Biotechnol.* **26**, 695-701.
- Mizuno, T., Yamaha, E., Kuroiwa, A. and Takeda, H. (1999). Removal of vegetal yolk causes dorsal deficiencies and impairs dorsal-inducing ability of the yolk cell in zebrafish. *Mech. Dev.* **81**, 51-63.
- Mowry, K. L. and Cote, C. A. (1999). RNA sorting in *Xenopus* oocytes and embryos. *FASEB J.* **13**, 435-445.
- Nojima, H., Rothamel, S., Shimizu, T., Kim, C. H., Yonemura, S., Marlow, F. L. and Hibi, M. (2010). Syntabulin, a motor protein linker, controls dorsal determination. *Development* **137**, 923-933.

- Ober, E. A. and Schulte-Merker, S.** (1999). Signals from the yolk cell induce mesoderm, neuroectoderm, the trunk organizer, and the notochord in zebrafish. *Dev. Biol.* **215**, 167-181.
- Paris, J. and Philippe, M.** (1990). Poly(A) metabolism and polysomal recruitment of maternal mRNAs during early *Xenopus* development. *Dev. Biol.* **140**, 221-224.
- Pei, W., Williams, P. H., Clark, M. D., Stemple, D. L. and Feldman, B.** (2007). Environmental and genetic modifiers of squint penetrance during zebrafish embryogenesis. *Dev. Biol.* **308**, 368-378.
- Pelegri, F.** (2003). Maternal factors in zebrafish development. *Dev. Dyn.* **228**, 535-554.
- Rebagliati, M. R., Toyama, R., Fricke, C., Haffter, P. and Dawid, I. B.** (1998). Zebrafish nodal-related genes are implicated in axial patterning and establishing left-right asymmetry. *Dev. Biol.* **199**, 261-272.
- Robu, M. E., Larson, J. D., Nasevicius, A., Beiraghi, S., Brenner, C., Farber, S. A. and Ekker, S. C.** (2007). p53 activation by knockdown technologies. *PLoS Genet.* **3**, e78.
- Sagata, N., Shiokawa, K. and Yamana, K.** (1980). A study on the steady-state population of poly(A)+RNA during early development of *Xenopus laevis*. *Dev. Biol.* **77**, 431-448.
- Sampath, K., Rubinstein, A. L., Cheng, A. M., Liang, J. O., Fekany, K., Solnica-Krezel, L., Korzh, V., Halpern, M. E. and Wright, C. V.** (1998). Induction of the zebrafish ventral brain and floorplate requires cyclops/nodal signalling. *Nature* **395**, 185-189.
- Schroeder, K. E., Condic, M. L., Eisenberg, L. M. and Yost, H. J.** (1999). Spatially regulated translation in embryos: asymmetric expression of maternal Wnt-11 along the dorsal-ventral axis in *Xenopus*. *Dev. Biol.* **214**, 288-297.
- Schulte-Merker, S., Hammerschmidt, M., Beuchle, D., Cho, K. W., De Robertis, E. M. and Nusslein-Volhard, C.** (1994). Expression of zebrafish goosecoid and no tail gene products in wild-type and mutant no tail embryos. *Development* **120**, 843-852.
- St Johnston, D.** (1995). The intracellular localization of messenger RNAs. *Cell* **81**, 161-170.
- Tao, Q., Yokota, C., Puck, H., Kofron, M., Birsoy, B., Yan, D., Asashima, M., Wylie, C. C., Lin, X. and Heasman, J.** (2005). Maternal wnt11 activates the canonical wnt signaling pathway required for axis formation in *Xenopus* embryos. *Cell* **120**, 857-871.
- Varnum, S. M. and Wormington, W. M.** (1990). Deadenylation of maternal mRNAs during *Xenopus* oocyte maturation does not require specific cis-sequences: a default mechanism for translational control. *Genes Dev.* **4**, 2278-2286.
- Westerfield, M.** (2007). *The Zebrafish Book. A Guide for the Laboratory Use of Zebrafish (Danio rerio)*, 5th edn. Eugene, OR: University of Oregon Press.
- Wylie, C., Kofron, M., Payne, C., Anderson, R., Hosobuchi, M., Joseph, E. and Heasman, J.** (1996). Maternal beta-catenin establishes a 'dorsal signal' in early *Xenopus* embryos. *Development* **122**, 2987-2996.
- Yamanaka, Y., Mizuno, T., Sasai, Y., Kishi, M., Takeda, H., Kim, C. H., Hibi, M. and Hirano, T.** (1998). A novel homeobox gene, dharma, can induce the organizer in a non-cell-autonomous manner. *Genes Dev.* **12**, 2345-2353.
- Zhang, J. and King, M. L.** (1996). *Xenopus* VegT RNA is localized to the vegetal cortex during oogenesis and encodes a novel T-box transcription factor involved in mesodermal patterning. *Development* **122**, 4119-4129.